Symmetric nuclear matter from the strong interaction

M. Leonhardt,[1] M. Pospiech,[1] B. Schallmo,[1] J. Braun,[1,2] C. Drischler,[3,4] K. Hebeler,[1,2] and A. Schwenk[1,2,5]

[1]*Institut für Kernphysik, Technische Universität Darmstadt, D-64289 Darmstadt, Germany*
[2]*ExtreMe Matter Institute EMMI, GSI, Planckstraße 1, D-64291 Darmstadt, Germany*
[3]*Department of Physics, University of California, Berkeley, CA 94720*
[4]*Lawrence Berkeley National Laboratory, Berkeley, CA 94720*
[5]*Max-Planck-Institut für Kernphysik, Saupfercheckweg 1, 69117 Heidelberg, Germany*

We study the equation of state of symmetric nuclear matter at zero temperature over a wide range of densities using two complementary theoretical approaches. At low densities up to twice nuclear saturation density, we compute the energy per particle based on modern nucleon-nucleon and three-nucleon interactions derived within chiral effective field theory. For higher densities we derive for the first time constraints in a Fierz-complete setting directly based on quantum chromodynamics using functional renormalization group techniques. We find remarkable consistency of the results obtained from both approaches as they come together in density and the natural emergence of a maximum in the speed of sound c_S at supranuclear densities. The presence of this maximum appears tightly connected to the formation of a diquark gap. Notably, this maximum is observed to exceed the asymptotic value $c_S^2 = 1/3$ while its exact position in terms of the density cannot yet be determined conclusively.

Introduction.– The theoretical understanding of the equation of state (EOS) of dense matter has been one of the main frontiers in nuclear physics in recent decades. While the EOS of cold matter up to around nuclear saturation density, $n_0 = 0.16\,\mathrm{fm}^{-3}$, can be constrained by properties of atomic nuclei [1–4], the composition and properties of matter at supranuclear densities as it exists, e.g., in the center of neutron stars are still open questions. Recent breakthroughs like the first detection of the gravitational wave signal of the neutron star merger [5, 6] as well as ongoing missions aiming at first direct neutron star radius measurements using x-ray timing [7–9] can significantly enhance our theoretical understanding of neutron-rich matter under extreme conditions. Combining information from these ongoing efforts with existing observational data like precise mass measurements of heavy neutron stars [10–13] or also heavy ion collisions [14] can provide further constraints for the EOS. However, all such measurements can only provide indirect insight into the microscopic nature of matter at high densities [15–17]. The present work aims to constrain properties of symmetric nuclear matter from calculations based on strong interactions with controlled uncertainties, without taking into account electromagnetic or weak interactions. This provides us with an insight into the composition of dense matter which, of course, eventually needs to be benchmarked against observational constraints.

Low-density regime.– At the fundamental level the strong interaction is governed by the quark-gluon dynamics described by quantum chromodynamics (QCD). At nuclear densities, the ground state is dominated by chiral symmetry breaking and calculations directly based on QCD become very challenging. For this regime chiral effective field theory (EFT) represents a powerful framework to describe the nuclear dynamics and interactions within a systematic expansion based on the low-energy degrees of freedom, nucleons and pions [18, 19]. Substantial progress has been achieved in recent years in deriving new nuclear forces and computing the EOS microscopically based on nucleon-nucleon (NN), three-nucleon (3N) and four-nucleon (4N) interactions derived within chiral EFT [20–29], see Ref. [30] for a recent review. In particular, in Ref. [29] we presented an efficient framework to compute the energy of nuclear matter at zero temperature within many-body perturbation theory (MBPT) up to high orders in the many-body expansion and for general proton fractions. It allows to include all contributions from two- and many-body forces up to N^{3}LO and to explore the connection of properties of matter and nuclei [31]. In addition, in Ref. [21] a set of NN and 3N interactions was fitted to few-body observables, where all derived interactions led to good saturation properties without adjustment of free parameters. In particular, one interaction of this set was found to also correctly predict the ground state energies of medium-mass nuclei up to ^{100}Sn [32, 33]. In Figs. 1 and 2, we show the results for the pressure and the speed of sound of symmetric nuclear matter up to twice nuclear density based on the set of interactions of Ref. [21] (individual blue lines) as well as the interactions up to N^{3}LO fitted to the empirical saturation point of Ref. [29] (blue bands). The EFT uncertainty bands at N^{2}LO (light-blue band) and N^{3}LO (dark-blue band) have been determined following the strategy of Ref. [34] and represent the combined uncertainties based on the results at the two cutoff scales $\Lambda = 450$ and 500 MeV (see also Ref. [29]).

Intermediate-density regime.– Compared to the nuclear density regime, less is known about the ground state at intermediate densities, i.e., the regime above the region where calculations based on chiral EFT are applicable and below the very high densities limit expected to be governed, e.g., by the formation of a diquark gap [35–41], or accessible by perturbative QCD (pQCD) at asymptotic densities [42–46]. To study the intermediate-density regime, we employ the functional renormalization group

(FRG) approach [47] which allows us to study this regime from the Euclidean QCD action (see Refs. [48–50] for reviews):

$$S = \int \mathrm{d}^4x \left\{ \frac{1}{4} F^a_{\mu\nu} F^a_{\mu\nu} + \bar{\psi} \left(\mathrm{i}\partial\!\!\!/ + \bar{g} A\!\!\!/ + \mathrm{i}\gamma_0 \mu \right) \psi \right\} . \quad (1)$$

Here, $\bar{g}$ is the bare gauge coupling and μ is the quark chemical potential. The non-Abelian fields A^a_μ enter the definition of the field-strength tensor $F^a_{\mu\nu}$ and are associated with the gluons. With respect to the quarks, we restrict ourselves to two massless flavors in this work.

In the RG flow, the quark-gluon vertex in Eq. (1) induces quark self-interactions already at the one-loop level via two-gluon exchange. This gives rise to terms, e.g., of the following form in the quantum effective action:

$$\delta\Gamma = \int \mathrm{d}^4x \, \bar{\lambda}_i (\bar{\psi}\mathcal{O}_i\psi)^2 \, , \quad (2)$$

where the operator $\mathcal{O}_i$ determines the color, flavor, and Dirac structure of the vertex. We stress that the four-quark couplings $\bar{\lambda}_i$ are not free parameters but solely generated by quark-gluon dynamics from first principles in our study. This is an important difference to, e.g., Nambu-Jona-Lasinio-type model studies where the four-quark couplings are input parameters, or to RG studies [35, 51] which expand the effective degrees of freedom around the Fermi surface in momentum space, thus being difficult to directly connect to the fundamental quark-gluon dynamics and the RG flow of the gauge coupling. In this work, we focus on the RG flow of pointlike projected four-quark correlation functions $\Gamma^{(4)}$. To be specific, we define the four-quark couplings associated with the vertex of the form (2) as follows

$$\begin{aligned} &\bar{\lambda}_i (\bar{\psi}\mathcal{O}_i\psi)^2 \quad (3) \\ &= \lim_{p_i \to 0} \bar{\psi}_\alpha(p_1)\bar{\psi}_\beta(p_2)\Gamma^{(4),\alpha\beta\gamma\delta}_{\mathcal{O}}(p_1,p_2,p_3,p_4)\psi_\gamma(p_3)\psi_\delta(p_4). \end{aligned}$$

Here, $\alpha, \beta, \gamma, \delta$ denote collective indices for color, flavor, and Dirac structures. Note that this zero-momentum projection does not represent a Silver-Blaze-symmetric point [52–54], but it matches the definition of four-quark couplings in conventional low-energy models [55–57] and BCS-type models [58–61]. The couplings resulting from our definition (3) depend on the chemical potential and the RG scale. Although this scale dependence implies that part of the momentum-dependent information is still taken into account in our RG analysis in an effective manner [62], the pointlike limit ignores relevant information of four-quark correlation functions. For example, bound-state information is encoded in the momentum structure of these correlation functions. Therefore, the pointlike approximation only allows us to study the symmetric high-energy regime [50]. The symmetry-broken low-energy regime is not accessible in this way. For our present purposes, however, this is still sufficient as it enables us to study the approach towards the symmetry-broken low-energy regime, as indicated by rapidly growing four-quark couplings.

In general, symmetry breaking is ultimately triggered by a specific four-quark channel approaching criticality as indicated by a divergence of the corresponding coupling. Such a seeming Landau-pole-type behavior of four-quark couplings can be traced back to the formation of condensates as they can be shown to be proportional to the inverse mass parameter of a Ginzburg-Landau effective potential for the order parameters in a (partially) bosonized formulation, $\lambda \sim 1/m^2$, see Refs. [50, 63, 64]. On the one hand, this implies that if the size of all four-quark couplings is found to be bounded, the system stays in the symmetric regime [50, 62, 65–67]. On the other hand, the observation of a rapidly growing four-quark coupling in a specific regime may be considered as an indicator that the order-parameter potential develops a non-zero ground-state expectation value in the direction associated with a specific four-quark channel. The nontrivial assumption entering our analysis of the EOS below is then that it is possible to relate the dominance pattern of the four-quark couplings to the symmetry-breaking pattern in terms of condensates, see Refs. [54, 62, 68, 69] for a detailed discussion. For example, in the zero-density limit, it has indeed been found that the scalar-pseudoscalar channel is the most dominant channel [70, 71] and a corresponding condensate is formed [71, 72] governing the low-energy dynamics.

When the baryon chemical potential is varied, it is reasonable to expect that the symmetry-breaking patterns associated with the various four-quark channels change. More specifically, channels other than the scalar-pseudoscalar channel may become relevant. In general, the most dominant channel can be identified by requiring that the modulus of the coupling of this channel is greater than the ones of the other four-quark couplings. Such an analysis then naturally requires to include all linearly-independent four-quark interactions permitted by the $SU(N_\mathrm{c}) \otimes SU_\mathrm{L}(2) \otimes SU_\mathrm{R}(2) \otimes U_\mathrm{V}(1)$ symmetry. Taking into account the explicit breaking of Poincaré and charge-conjugation invariance at finite density, we end up with a Fierz-complete basis set composed of ten channels in the pointlike limit [68]. All other channels are related to this minimal basis by means of Fierz transformations.

Introducing the dimensionless renormalized four-quark couplings $\lambda_i = k^2\bar{\lambda}_i$ with k being the RG scale, the β functions for these couplings can be written in the following form:

$$k\partial_k\lambda_i = 2\lambda_i - \lambda_j A^{(i)}_{jk}\lambda_k - B^{(i)}_j \lambda_j g^2 - C^{(i)} g^4, \quad (4)$$

where i refers to the elements of our Fierz-complete basis of four-quark couplings. The coefficients A (purely fermionic loop), B (triangle diagram), and C (two-gluon exchange) depend on the quark chemical potential. Here, we have dropped an implicit dependence of these loop diagrams on the wavefunction renormalization factors of the quarks and the gluons as they have been found to be subleading in the symmetric regime [65–67, 73, 74]. For the computation of the flow equations (4), we have then made use of existing software packages [75, 76]. For de-

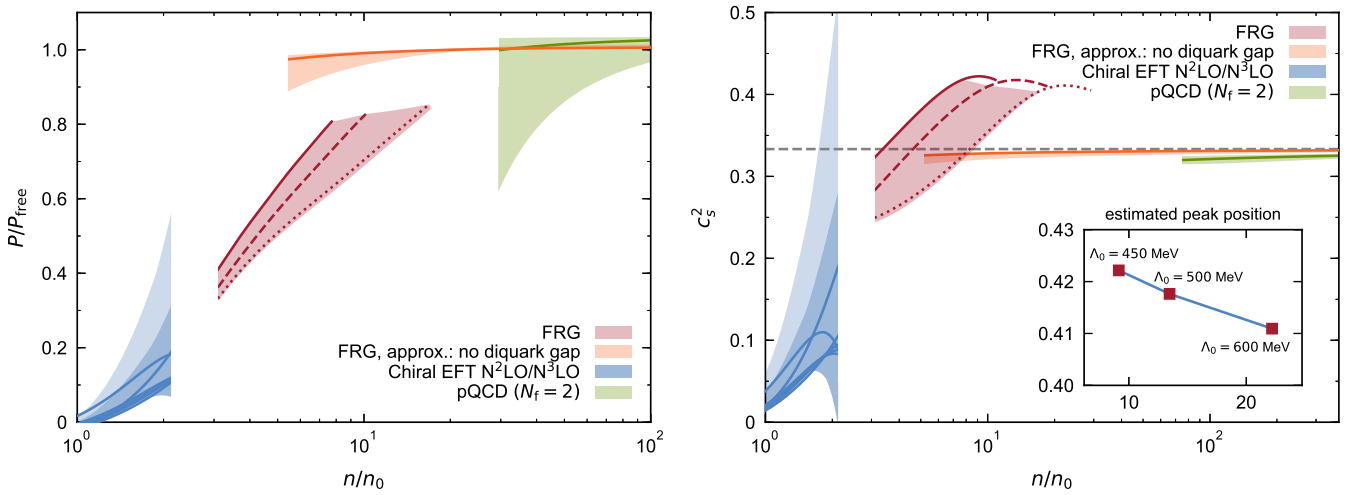

Figure 1: Left panel: Pressure P of symmetric nuclear matter normalized by the pressure of the free quark gas $P_{\rm SB}$ as a function of the baryon density n/n_0 in units of the nuclear saturation density as obtained from chiral EFT, FRG, including results from an approximation without taking into account a diquark gap (FRG, approx.: no diquark gap), and pQCD, see main text for details. Right panel: Speed of sound squared as a function of the baryon density in units of the nuclear saturation density as derived from the pressure shown in the left panel. The inset shows the estimated peak position and height for different transition scales Λ_0 as obtained by increasing the chemical potential μ beyond Λ_0.

tails we refer the reader to Ref. [77]. The corresponding flow equations for the purely fermionic part as parameterized by the matrices $A^{(i)}$ can be found in Ref. [68], including a discussion of the regularization scheme also underlying this work.

In our present study, the RG flow of the gauge sector enters the flow equations of the four-quark couplings only via the running of the strong coupling. In line with our approximations in the computation of the four-quark couplings, we only employ the one-loop running of the strong coupling for two quark flavors. However, we have checked that our main results (e.g., the existence of a maximum in the speed of sound) persist even if we employ running couplings taking into account higher-order effects [66, 67, 78]. Note that from the analysis of Ward-Takahashi identities, it follows that the back-reaction of the four-quark couplings on the strong coupling is negligible, provided the flow of the four-quark couplings is governed by the presence of fixed points [74], as it is the case in the symmetric regime [65–67].

Using the set of flow equations defined by Eq. (4), we can study the RG flow of the four-quark couplings and analyze the emerging symmetry breaking patterns. At high-energy scales, the RG flow generates quark self-interactions $\lambda_i \sim g^4$ via the last term in Eq. (4). Following the RG flow towards the low-energy regime, we observe that the strength of the four-quark couplings relative to each other depends on the dimensionless quark chemical potential μ. More specifically, towards lower density, the most dominant channel in the low-energy regime eventually turns out to be the scalar-pseudoscalar channel, in line with phenomenological expectations. As also observed in Ref. [68], the dominance pattern changes when the dimensionless chemical potential μ/k becomes sufficiently large. Then, the diquark channel $\sim \left(\mathrm{i}\bar{\psi}\gamma_5\tau_2 T^A \psi^C\right)\left(\mathrm{i}\bar{\psi}^C\gamma_5\tau_2 T^A \psi\right)$ (where τ_2 is the second antisymmetric Pauli matrix and it is only summed over the antisymmetric color generators T^A) takes over the role of the most dominant channel, suggesting the formation of a chirally symmetric diquark condensate associated with pairing of the two-flavor color-superconductor (2SC) type [36–41]. Note that in case of electromagnetic neutrality and β equilibrium the inclusion of strange quarks entails also different pairing patterns such as the color-flavor-locked pairing present at least at very high densities [79].

For a computation of the EOS, it is required to solve the RG flow down to the long-range limit $k \to 0$. As discussed above, however, this requires to go beyond the pointlike limit and resolve the momentum dependencies of the corresponding vertices. For example, this can be conveniently done by employing so-called dynamical hadronization techniques [48, 64, 73, 80], see, e.g., Refs. [71, 72, 78, 81] for their application to QCD. These techniques effectively implement continuous Hubbard-Stratonovich transformations of four-quark interactions in the RG flow. In the present work, we do not employ continuous transformations but essentially perform them at a given scale Λ_0 [82]. To be specific, for any given μ, we follow the RG flow of the four-quark couplings from the perturbative high-energy regime down to the scale Λ_0 at which we extract the strength of the four-quark couplings and use them to fix the couplings of an ansatz describing the dynamics at scales $k < \Lambda_0$. Since we find the scalar-pseudoscalar channel to be most dominant at low densities and the diquark channel to be

most dominant at intermediate and high densities, in accordance with the findings in Ref. [51], we parametrize the low-energy regime associated with scales $k \leq \Lambda_0$ by the Hubbard-Stratonovich transforms of these two couplings cast into the form of a quark-meson-diquark-model truncation. From the latter, we then compute the pressure via a minimization of the corresponding Ginzburg-Landau-type effective potential [83] spanned by the aforementioned two Hubbard-Stratonovich fields in an RG-consistent way, see Ref. [84] for details.

To set the scale, we fix the actual value of the scalar-pseudoscalar coupling of the low-energy sector by the constituent quark mass in the vacuum limit. The value of the diquark coupling relative to the scalar-pseudoscalar coupling is then fixed by the corresponding ratio obtained from our RG flow study of gluon-induced four-quark interactions evaluated at the scale Λ_0. Because the gluon-induced four-quark interactions depend on the quark chemical potential, this renders the couplings of the low-energy regime μ-dependent. Finally, to estimate the uncertainties arising from the presence of the scale Λ_0 describing the "transition" in the effective degrees of freedom, we vary this scale from $\Lambda_0 = 450 \ldots 600\,\mathrm{MeV}$.

In the left panel of Fig. 1, we show our results for the EOS (light-red band) as a function of the baryon density in units of the nuclear saturation density. The band has been obtained from a variation of the scale Λ_0 and a variation of the value of the gauge coupling within experimental errors at the initial RG scale [85]. The different line types within the light-red band depict three representative EOSs associated with $\Lambda_0 = 450, 500, 600\,\mathrm{MeV}$ (from left to right). At lower densities, we observe that our results for the pressure as obtained from our many-body framework based on chiral EFT interactions are remarkably consistent with those obtained from our FRG analysis at intermediate densities. However, our present approximation is not capable to resolve the exact position of any chiral transition or crossover as we do not observe a clear dominance pattern in the spectrum of the four-quark couplings in this regime. The extent of the light-red band at high densities is set by the constraint $\mu \leq \Lambda_0$. With respect to the high-density limit, we note that the results from our FRG studies are found to approach those from pQCD calculations (light-green band) [45, 46].

In the right panel of Fig. 1, we present the square of the speed of sound as a function of the baryon density n as derived from the pressure shown in the left panel. The light-red band is associated with the results from our FRG studies taking diquark condensation into account. Its extent to high densities is again constrained by the "transition" scale Λ_0. Irrespective of this limitation of our present study, a softening of the EOS at high densities may in general be expected from a perturbative standpoint as associated with an evaluation of, e.g., the four-quark couplings at the characteristic scale $\mu \sim n^{\frac{1}{3}}$. In fact, at large chemical potential, the four-quark couplings λ_i then naturally become small owing to asymptotic freedom, $\lambda_i \sim g^4$, see also Eq. (4). Even more, according to pQCD studies [42–46], we expect the speed of sound to approach $c_\mathrm{s}^2 = 1/3$ (non-interacting limit) from below at asymptotically high densities. From this and our observation that the pressure exceeds its asymptotic value already for chemical potentials well below the scale Λ_0, we infer the existence of a maximum in the speed of sound. In order to also give an estimate for the position and height of the maximum, we may increase the chemical potential μ beyond Λ_0 in our calculations. The inset of this figure shows the resulting estimate, exhibiting a robust height of the maximum but with a large uncertainty of its position. At high density, $n/n_0 > 75$, we show again results from pQCD calculations. Note that the computation of the speed of sound from the corresponding data for the pressure in this high-density branch becomes numerically unstable for $n/n_0 \lesssim 70$.

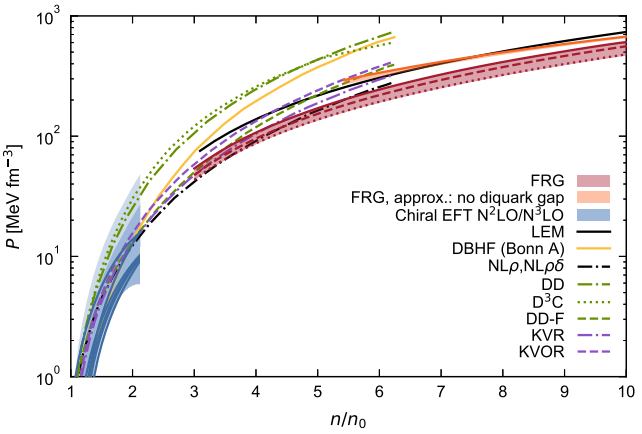

Figure 2: Pressure of symmetric nuclear matter as obtained from chiral EFT, FRG, and pQCD, as in Fig. 1, in comparison with different models (see main text and also Ref. [86]).

Besides pressure and speed of sound, the diquark gap Δ is of great relevance for dense matter physics [60]. In our present study, we observe that Δ increases within the considered density range $n/n_0 \approx 2 \ldots 15$, exhibiting a flattening towards higher densities. More specifically, we find that Δ is greater than the values reported in Ref. [37]. However, the values for Δ from both studies show a remarkable agreement at lower densities. For $n/n_0 \approx 5$, for example, we extract $\Delta \approx 70 \ldots 160\,\mathrm{MeV}$ from Ref. [37] and $\Delta \approx 140 \ldots 230\,\mathrm{MeV}$ (depending on Λ_0) from our present study.

In Fig. 2, we next compare our results for the pressure with different models. These include relativistic mean-field calculations, such as NLρ and NL$\rho\delta$ [87], DD, D^{3}C and DD-F [88] as well as KVR and KVOR [89] (see also Ref. [86]). In addition, we show results of Dirac-Brueckner Hartree-Fock calculations (DBHF) [90] and from a typical low-energy model (LEM) [56, 84]. At densities up to around twice nuclear saturation density, the different models are compatible with the chiral EFT uncertainty bands at N^{2}LO (but not all at N^{3}LO). At higher

densities, however, the pressure obtained from most models is found to be significantly higher than our results.

High-density regime.– In the regime of very high densities the EOS can be calculated using perturbative methods [42–46] owing to the fact that the dynamics is dominated by modes with momenta $|p| \sim \mu$ which effectively renders the QCD coupling $g^2/4\pi$ small. Although the ground state is expected to be governed by diquark condensation [35–37, 39–41], calculations that do not include condensation effects are reliable, provided that the chemical potential is much larger than the scale set by the diquark gap.

In our RG study, the gluon-induced four-quark interactions serve as proxies for the various order parameters. The analysis of their RG flows indeed indicate that the ground state is governed by spontaneous symmetry breaking, even at high densities. This can be effectively described by a transition in the relevant degrees of freedom at a finite scale. In order to make contact with perturbative calculations, we drop the running of the four-quark interactions and restrict ourselves to the running of the quark and gluon wavefunction renormalization factors at leading order in the derivative expansion. From the latter, we obtain dressed quark and gluon propagators which are then used to compute the pressure. In this case, we find that the RG flow of the pressure can be followed from high-energy scales down to the deep infrared limit without encountering any pairing instabilities as associated with spontaneous symmetry breaking. In Fig. 1, we show our results for the pressure and the speed of sound from this calculation labelled "no diquark gap". We observe very good agreement with recent perturbative calculations [45, 46]. The width of the orange FRG band illustrates the uncertainty arising from a variation of the regularization scheme and a variation of the running gauge coupling within the experimental error bars at the τ-mass scale [85]. Following the pressure towards smaller densities, we observe that our results for the intermediate-density and high-density regime are consistent. For the appearance of a maximum in the speed of sound, however, we find that the inclusion of condensation effects in the regime $n/n_0 \lesssim 30$ is crucial, which also provides the necessary decrease of the pressure in order to connect the low-density with the high-density regime.

Conclusions and Outlook.– In this Letter we have presented first results for the EOS of symmetric nuclear matter at zero temperature over a wide density range starting from QCD. At low densities we performed calculations based on a set of recently developed chiral NN and 3N interactions, while for densities beyond three times saturation density we computed the EOS within an FRG framework directly based on the fundamental quark-gluon dynamics. Even though the present approximations underlying both studies break down at an intermediate-density window, the results show a remarkable consistency (in particular for the pressure) and indicate that they can be combined via simple extrapolations. At intermediate to high densities, our study suggests that the ground state is governed by diquark dynamics. From a combined analysis of our results and those from perturbative studies, we infer the existence of a maximum in the speed of sound. Although the exact position of this maximum in terms of the density cannot be determined conclusively in our present study, its height appears very robust. Note that the existence of a maximum for the speed of sound has also been demonstrated for neutron-rich matter based on constraints from neutron star masses [91–94]. Ignoring the diquark gap, our FRG calculations are then found to be in good agreement with well-known results from pQCD calculations at very high densities. A generalization of the presented framework to general proton fractions will give us access to the EOS in the neutron-rich regime, which is relevant for astrophysical applications. Furthermore, the FRG approach is already formulated for general temperatures. An extension of our chiral EFT calculations at low densities to finite temperatures will allow us to also study the temperature dependence of the EOS over a wide density range based on strong interactions.

Acknowledgments.– This work is supported in part by the Deutsche Forschungsgemeinschaft (DFG, German Research Foundation) – Projektnummer 279384907 – SFB 1245, the US Department of Energy, the Office of Science, the Office of Nuclear Physics, and SciDAC under awards DE_SC00046548 and DE_AC02_05CH11231. J.B. acknowledges support by the DFG under grant BR 4005/4-1 (Heisenberg program) and by HIC for FAIR within the LOEWE program of the State of Hesse. C.D. acknowledges support by the Alexander von Humboldt Foundation through a Feodor-Lynen Fellowship. Computational resources have been provided by the Lichtenberg high performance computer of the TU Darmstadt. J.B., M.L., and M.P. as members of the fQCD collaboration [95] would like to thank the other members of this collaboration for discussions and providing data for cross-checks.

[1] M. B. Tsang *et al.*, Phys. Rev. C **86**, 015803 (2012), arXiv:1204.0466 [nucl-ex] .
[2] J. M. Lattimer and Y. Lim, Astrophys. J. **771**, 51 (2013), arXiv:1203.4286 [nucl-th] .
[3] K. Hebeler, J. D. Holt, J. Menendez, and A. Schwenk, Ann. Rev. Nucl. Part. Sci. **65**, 457 (2015), arXiv:1508.06893 [nucl-th] .
[4] X. Roca-Maza and N. Paar, Prog. Part. Nucl. Phys. **101**, 96 (2018), arXiv:1804.06256 [nucl-th] .
[5] B. P. Abbott *et al.* (LIGO Scientific, Virgo), Phys. Rev. Lett. **119**, 161101 (2017), arXiv:1710.05832 [gr-qc] .
[6] B. P. Abbott *et al.* (LIGO Scientific, Virgo), Phys. Rev. X **9**, 011001 (2019), arXiv:1805.11579 [gr-qc] .
[7] A. L. Watts *et al.*, Rev. Mod. Phys. **88**, 021001 (2016),

arXiv:1602.01081 [astro-ph.HE] .

[8] Z. Arzoumanian *et al.*, in *Space Telescopes and Instrumentation 2014: Ultraviolet to Gamma Ray*, Proc. SPIE, Vol. 9144 (2014) p. 914420.

[9] K. C. Gendreau *et al.*, in *Space Telescopes and Instrumentation 2016: Ultraviolet to Gamma Ray*, Proc. SPIE, Vol. 9905 (2016) p. 99051H.

[10] P. Demorest, T. Pennucci, S. Ransom, M. Roberts, and J. Hessels, Nature **467**, 1081 (2010).

[11] J. Antoniadis *et al.*, Science **340**, 448 (2013), arXiv:1304.6875 [astro-ph.HE] .

[12] E. Fonseca *et al.*, Astrophys. J. **832**, 167 (2016).

[13] H. T. Cromartie *et al.*, Nature Astronomy **4**, 72 (2020), arXiv:1904.06759 [astro-ph.HE] .

[14] P. Danielewicz, R. Lacey, and W. G. Lynch, Science **298**, 1592 (2002), nucl-th/0208016 .

[15] A. W. Steiner, J. M. Lattimer, and E. F. Brown, Astrophys. J. **722**, 33 (2010), arXiv:1005.0811 [astro-ph.HE] .

[16] K. Hebeler, J. M. Lattimer, C. J. Pethick, and A. Schwenk, Astrophys. J. **773**, 11 (2013), arXiv:1303.4662 [astro-ph.SR] .

[17] F. Özel and P. Freire, Ann. Rev. Astron. Astrophys. **54**, 401 (2016), arXiv:1603.02698 [astro-ph.HE] .

[18] E. Epelbaum, H.-W. Hammer, and U.-G. Meißner, Rev. Mod. Phys. **81**, 1773 (2009), arXiv:0811.1338 [nucl-th] .

[19] R. Machleidt and D. R. Entem, Phys. Rept. **503**, 1 (2011), arXiv:1105.2919 [nucl-th] .

[20] K. Hebeler and A. Schwenk, Phys. Rev. C **82**, 014314 (2010), arXiv:0911.0483 [nucl-th] .

[21] K. Hebeler, S. K. Bogner, R. J. Furnstahl, A. Nogga, and A. Schwenk, Phys. Rev. C **83**, 031301 (2011), arXiv:1012.3381 [nucl-th] .

[22] I. Tews, T. Krüger, K. Hebeler, and A. Schwenk, Phys. Rev. Lett. **110**, 032504 (2013), arXiv:1206.0025 [nucl-th] .

[23] G. Hagen, T. Papenbrock, A. Ekström, K. A. Wendt, G. Baardsen, S. Gandolfi, M. Hjorth-Jensen, and C. J. Horowitz, Phys. Rev. C **89**, 014319 (2014), arXiv:1311.2925 [nucl-th] .

[24] A. Carbone, A. Rios, and A. Polls, Phys. Rev. C **88**, 044302 (2013), arXiv:1307.1889 [nucl-th] .

[25] L. Coraggio, J. W. Holt, N. Itaco, R. Machleidt, L. E. Marcucci, and F. Sammarruca, Phys. Rev. C **89**, 044321 (2014), arXiv:1402.0965 [nucl-th] .

[26] C. Wellenhofer, J. W. Holt, and N. Kaiser, Phys. Rev. C **92**, 015801 (2015), arXiv:1504.00177 [nucl-th] .

[27] J. E. Lynn, I. Tews, J. Carlson, S. Gandolfi, A. Gezerlis, K. E. Schmidt, and A. Schwenk, Phys. Rev. Lett. **116**, 062501 (2016), arXiv:1509.03470 [nucl-th] .

[28] C. Drischler, K. Hebeler, and A. Schwenk, Phys. Rev. C **93**, 054314 (2016), arXiv:1510.06728 [nucl-th] .

[29] C. Drischler, K. Hebeler, and A. Schwenk, Phys. Rev. Lett. **122**, 042501 (2019), arXiv:1710.08220 [nucl-th] .

[30] K. Hebeler, (2020), arXiv:2002.09548 [nucl-th] .

[31] J. Hoppe, C. Drischler, K. Hebeler, A. Schwenk, and J. Simonis, Phys. Rev. C **100**, 024318 (2019), arXiv:1904.12611 [nucl-th] .

[32] J. Simonis, S. R. Stroberg, K. Hebeler, J. D. Holt, and A. Schwenk, Phys. Rev. C **96**, 014303 (2017), arXiv:1704.02915 [nucl-th] .

[33] T. D. Morris, J. Simonis, S. R. Stroberg, C. Stumpf, G. Hagen, J. D. Holt, G. R. Jansen, T. Papenbrock, R. Roth, and A. Schwenk, Phys. Rev. Lett. **120**, 152503 (2018), arXiv:1709.02786 [nucl-th] .

[34] E. Epelbaum, H. Krebs, and U.-G. Meißner, Eur. Phys. J. **A51**, 53 (2015), arXiv:1412.0142 [nucl-th] .

[35] D. T. Son, Phys. Rev. D **59**, 094019 (1999), hep-ph/9812287 .

[36] R. Rapp, T. Schäfer, E. V. Shuryak, and M. Velkovsky, Phys. Rev. Lett. **81**, 53 (1998), hep-ph/9711396 .

[37] M. G. Alford, K. Rajagopal, and F. Wilczek, Phys. Lett. **B422**, 247 (1998), hep-ph/9711395 [hep-ph] .

[38] J. Berges and K. Rajagopal, Nucl. Phys. **B538**, 215 (1999), hep-ph/9804233 .

[39] R. D. Pisarski and D. H. Rischke, Phys. Rev. D **61**, 074017 (2000), nucl-th/9910056 .

[40] R. D. Pisarski and D. H. Rischke, Phys. Rev. D **61**, 051501 (2000), nucl-th/9907041 .

[41] T. Schäfer and F. Wilczek, Phys. Rev. D **60**, 114033 (1999), hep-ph/9906512 .

[42] B. A. Freedman and L. D. McLerran, Phys. Rev. D **16**, 1130 (1977).

[43] B. A. Freedman and L. D. McLerran, Phys. Rev. D **16**, 1169 (1977).

[44] V. Baluni, Phys. Rev. D **17**, 2092 (1978).

[45] A. Kurkela, P. Romatschke, and A. Vuorinen, Phys. Rev. D **81**, 105021 (2010), arXiv:0912.1856 [hep-ph] .

[46] T. Gorda, A. Kurkela, P. Romatschke, M. Säppi, and A. Vuorinen, Phys. Rev. Lett. **121**, 202701 (2018), arXiv:1807.04120 [hep-ph] .

[47] C. Wetterich, Phys. Lett. **B301**, 90 (1993), arXiv:1710.05815 [hep-th] .

[48] J. M. Pawlowski, Ann. Phys. **322**, 2831 (2007), hep-th/0512261 .

[49] H. Gies, Lect. Notes Phys. **852**, 287 (2012), hep-ph/0611146 .

[50] J. Braun, J. Phys. G **39**, 033001 (2012), arXiv:1108.4449 [hep-ph] .

[51] T. Schäfer and F. Wilczek, Phys. Lett. **B450**, 325 (1999), hep-ph/9810509 .

[52] N. Khan, J. M. Pawlowski, F. Rennecke, and M. M. Scherer, (2015), arXiv:1512.03673 [hep-ph] .

[53] W.-j. Fu, J. M. Pawlowski, F. Rennecke, and B.-J. Schaefer, Phys. Rev. D **94**, 116020 (2016), arXiv:1608.04302 [hep-ph] .

[54] J. Braun, M. Leonhardt, and M. Pospiech, Phys. Rev. D **96**, 076003 (2017), arXiv:1705.00074 [hep-ph] .

[55] S. P. Klevansky, Rev. Mod. Phys. **64**, 649 (1992).

[56] M. Buballa, Phys. Rept. **407**, 205 (2005), hep-ph/0402234 .

[57] K. Fukushima, J. Phys. G **39**, 013101 (2012), arXiv:1108.2939 [hep-ph] .

[58] D. Bailin and A. Love, Phys. Rept. **107**, 325 (1984).

[59] A. Altland and B. Simons, *Condensed matter field theory* (2006).

[60] M. G. Alford, A. Schmitt, K. Rajagopal, and T. Schäfer, Rev. Mod. Phys. **80**, 1455 (2008), arXiv:0709.4635 [hep-ph] .

[61] R. Anglani, R. Casalbuoni, M. Ciminale, N. Ippolito, R. Gatto, M. Mannarelli, and M. Ruggieri, Rev. Mod. Phys. **86**, 509 (2014), arXiv:1302.4264 [hep-ph] .

[62] J. Braun, H. Gies, L. Janssen, and D. Roscher, Phys. Rev. D **90**, 036002 (2014), arXiv:1404.1362 [hep-ph] .

[63] U. Ellwanger and C. Wetterich, Nucl. Phys. **B423**, 137 (1994), hep-ph/9402221 .

[64] H. Gies and C. Wetterich, Phys. Rev. **D65**, 065001

(2002), hep-th/0107221 .
[65] H. Gies and J. Jaeckel, Eur. Phys. J. **C46**, 433 (2006), hep-ph/0507171 .
[66] J. Braun and H. Gies, Phys. Lett. B **645**, 53 (2007), hep-ph/0512085 .
[67] J. Braun and H. Gies, JHEP **06**, 024 (2006), hep-ph/0602226 .
[68] J. Braun, M. Leonhardt, and M. Pospiech, Phys. Rev. D **97**, 076010 (2018), arXiv:1801.08338 [hep-ph] .
[69] D. Roscher, N. Gneist, M. M. Scherer, S. Trebst, and S. Diehl, (2019), arXiv:1905.01060 [cond-mat.str-el] .
[70] J. Braun, *Functional renormalization group methods in quantum chromodynamics*, Ph.D. thesis, Heidelberg U. (2006).
[71] M. Mitter, J. M. Pawlowski, and N. Strodthoff, Phys. Rev. D **91**, 054035 (2015), arXiv:1411.7978 [hep-ph] .
[72] A. K. Cyrol, M. Mitter, J. M. Pawlowski, and N. Strodthoff, Phys. Rev. D **97**, 054006 (2018), arXiv:1706.06326 [hep-ph] .
[73] H. Gies and C. Wetterich, Phys. Rev. **D69**, 025001 (2004), hep-th/0209183 .
[74] H. Gies, J. Jaeckel, and C. Wetterich, Phys. Rev. **D69**, 105008 (2004), hep-ph/0312034 .
[75] M. Q. Huber and J. Braun, Comput. Phys. Commun. **183**, 1290 (2012), arXiv:1102.5307 [hep-th] .
[76] A. K. Cyrol, M. Mitter, and N. Strodthoff, Comput. Phys. Commun. **219**, 346 (2017), arXiv:1610.09331 [hep-ph] .
[77] J. Braun, M. Leonhardt, and M. Pospiech, Phys. Rev. D **101**, 036004 (2020), arXiv:1909.06298 [hep-ph] .
[78] J. Braun, L. Fister, J. M. Pawlowski, and F. Rennecke, Phys. Rev. D **94**, 034016 (2016), arXiv:1412.1045 [hep-ph] .
[79] M. G. Alford, K. Rajagopal, and F. Wilczek, Nucl. Phys. **B537**, 443 (1999), hep-ph/9804403 .
[80] S. Floerchinger and C. Wetterich, Phys. Lett. B **680**, 371 (2009), arXiv:0905.0915 [hep-th] .
[81] J. Braun, Eur. Phys. J. C **64**, 459 (2009), arXiv:0810.1727 [hep-ph] .
[82] P. Springer, J. Braun, S. Rechenberger, and F. Rennecke, *Proceedings, 12th Conference on Quark Confinement and the Hadron Spectrum (Confinement XII): Thessaloniki, Greece*, EPJ Web Conf. **137**, 03022 (2017), arXiv:1611.06020 [hep-ph] .
[83] W.-j. Fu, J. M. Pawlowski, and F. Rennecke, (2018), arXiv:1808.00410 [hep-ph] .
[84] J. Braun, M. Leonhardt, and J. M. Pawlowski, SciPost Phys. **6**, 056 (2019), arXiv:1806.04432 [hep-ph] .
[85] S. Bethke, Eur. Phys. J. C **64**, 689 (2009), arXiv:0908.1135 [hep-ph] .
[86] T. Klähn *et al.*, Phys. Rev. C **74**, 035802 (2006), nucl-th/0602038 .
[87] B. Liu, V. Greco, V. Baran, M. Colonna, and M. Di Toro, Phys. Rev. C **65**, 045201 (2002), nucl-th/0112034 .
[88] S. Typel, Phys. Rev. C **71**, 064301 (2005), nucl-th/0501056 .
[89] E. E. Kolomeitsev and D. N. Voskresensky, Nucl. Phys. A **759**, 373 (2005), nucl-th/0410063 .
[90] E. N. E. van Dalen, C. Fuchs, and A. Faessler, Phys. Rev. C **72**, 065803 (2005), nucl-th/0511040 .
[91] P. Bedaque and A. W. Steiner, Phys. Rev. Lett. **114**, 031103 (2015), arXiv:1408.5116 [nucl-th] .
[92] I. Tews, J. Carlson, S. Gandolfi, and S. Reddy, Astrophys. J. **860**, 149 (2018), arXiv:1801.01923 [nucl-th] .
[93] S. K. Greif, G. Raaijmakers, K. Hebeler, A. Schwenk, and A. L. Watts, Mon. Not. Roy. Astron. Soc. **485**, 5363 (2019), arXiv:1812.08188 [astro-ph.HE] .
[94] E. Annala, T. Gorda, A. Kurkela, J. Nättilä, and A. Vuorinen, (2019), arXiv:1903.09121 [astro-ph.HE] .
[95] *fQCD Collaboration*, J. Braun, L. Corell, W.-j. Fu, C. Huang, M. Leonhardt, J. M. Pawlowski, M. Pospiech, F. Rennecke, D. Rosenblüh, C. Schneider, R. Wen, N. Wink, and S. Yin (members as of July 2019).